

Position and Suction Control of a Reconfigurable Robotic Gripper*

Nikos Tsourveloudis[†], Kimon P. Valavanis^{†,‡}, Ramesh Kolluru[‡], and Ioannis K. Nikolos[†]

Abstract: This paper discusses position and suction control of a multi-degree-of-freedom reconfigurable robotic gripper system (RGS) consisting of four arms in a crossbar configuration, with a flat surface, fixed dimensions, suction unit (cup) mounted on each of the four arms. A fuzzy logic based controller has been implemented to regulate, coordinate and maintain the amount of suction generated through each of the suction units and the positioning of the suction cups along each arm length. The RGS is integrated with AdeptOne and/or AdeptThree commercial manipulators and used to automate limp material handling, reliably, without distortion, deformation and/or folding. Extensive simulation results indicate that the RGS control system is robust, reliable and accurate, and meets a set of system requirements specified by the industry. A prototype system is being built, based on the derived design and model of the system.

Keywords: Reconfigurable, Robotic Gripper, Apparel Industry, Fuzzy Control

1. Introduction

THIS research is the outgrowth of previously reported work in the area of designing and prototyping robotic grippers for limp (deformable) material manipulation. The central objectives of such grippers are, first, the ability to manipulate single and/or multiple panels of varying shapes and sizes without material distortion, deformation and/or folding, and second, easy integration with commercially available robot manipulators [1]–[5], [12].

After a review and comparison of existing commercial and research limp material handling systems and gripping mechanisms (electrostatic, suction, thermal, chemical adhesion) [3], it was obvious that suction (due to its non-intrusive and non-incisive characteristics) offers high gripping strength, low cost and ease of implementation and it is the most appropriate mechanism to handle delicate deformable material. Therefore, as the first step, a prototype flat-surfaced, fixed-dimensions gripper system was built and integrated with AdeptOne and AdeptThree robot manipulators (**Fig. 1**). This first prototype gripper design consisted of a 9"×12" rectangular chamber with circular perforations on the pickup surface. The gripper used suction to handle material panels whose shape and size matched or were smaller than its dimensions. Design details and experimental performance evaluation have already been presented in [3].

However, in order to handle material panels of various shapes, sizes and weight, the multi-degree-of-freedom RGS of **Fig. 2** was designed, tested and integrated with AdeptOne and/or AdeptThree commercial manipulators. Industry requirements [12] dictated that the gripper has the

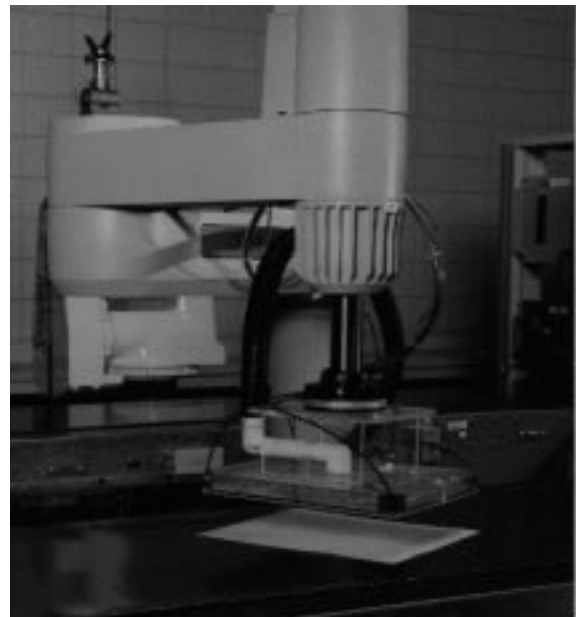


Fig. 1 The existing gripper system

ability to manipulate single and/or multiple panels of varying shapes and sizes (up to 36"×36") without material distortion, deformation and/or folding with a total payload capacity of 10 pounds.

The overall RGS control architecture has three modules, *the gripper system, the robot arm, and the suction generation system* as shown in **Fig. 3** (details are presented in [2], [4], [12]). The *enhanced robot controller* includes the AdeptOne or AdeptThree original controller and the interfaces built to integrate the reconfigurable gripper with the original robot controller.

Design constraints required that maximum stresses within the RGS be significantly smaller than its failure stress values, and the deflections be minimal so that RGS positioning accuracy and repeatability are maximized. An additional constraint, imposed by the 50 pound payload capacity of the AdeptThree-XL SCARA robot arm, dic-

* Received September 2, 1999; accepted November 12, 1999.

[†] Department of Production Engineering and Management, Technical University of Crete, 73100 Chania, Greece. E-mail: nikost@dpem.tuc.gr

[‡] Robotics and Automation Laboratory (RAL), The Center for Advanced Computer Studies (CACs), University of Southwestern Louisiana (USL), Lafayette, LA 70504, USA. E-mail: kimon@cac.s.usl.edu



Fig. 2 Design of the reconfigurable gripper system



Fig. 3 The reconfigurable gripper prototype mounted on an Adept robot arm

tated that the design of the RGS be such that its total self-weight is minimized to maximize effective payload capacity. Kinematics constraints required that the system be considered as a cantilever beam, fully constrained on one end, with point load (consisting of the gripper self-weight and external payload) acting on the free end of the cantilever. Static analysis [6] determined the likelihood of system failure due to fatigue stresses under load and kinematics constraints. Stresses developed and the deflections caused in the body due to the self-weight of the cantilever and external loads were calculated. Once the mechanism was proven to be statically robust, dynamic analysis of the mechanism was performed to evaluate the effect of accelerations of the robot arm on the dynamic displacements and the dynamic stresses generated within the RGS. Dynamic analysis [10] resulted in determining the mechanisms' natural frequency and system modes, and in evaluating the effects of dynamics of the robot arm on dynamic displacements and dynamic stresses generated within the mechanism. Theoretical analysis coupled by simulation-based verification using I-DEAS [11], resulted in a specific RGS design with accurately calculated design parameters [12] as shown in **Table 1**.

Table 1 Design parameters of the RGS

Length of each arm (L)	12 [in]	
Diameter of each arm (d)	0.5 [in]	
Payload on each arm	Max. 5 [lb]	
	Theoretical	Simulation
Maximum stress (Loaded)	5250 [lb/in ²]	5210 [lb/in ²]
Maximum deflections (Unloaded)	0.0015 [in]	0.00155 [in]
Maximum deflections (Loaded)	0.031 [in]	0.0329 [in]
Natural frequency of each arm	98.24 [rad/s]	104.77 [rad/s]
Damped frequency of each arm	98.73 [rad/s]	104.24 [rad/s]

Given the above constraints and determined design specification parameters, we focus on the control aspects of the multi-degree-of-freedom reconfigurable robotic gripper system (RGS), concentrating on the position and suction control modules shown in **Fig. 4**. Fuzzy control formalism is introduced for the positioning of the suction cups. A detailed discussion on the airflow is presented (needed to generate adequate grasping force through the suction cups) together with justifications for the use of knowledge-based methodologies for suction control.

2. Control Fundamentals

As shown in Fig. 2, the reconfigurable gripper consists of four arms in a crossbar configuration, with flat surfaced, fixed dimensions, suction unit (cup) mounted on each of the four arms. The suction cup may be translated along the length of the arm, which is a linear actuator drive mechanism. Each suction cup is a rectangular chamber with circular perforations on the bottom pickup surface.

The Adept robotic vision system is used to identify incoming panels and to calculate the center of gravity of the panel (object) and its second moments of inertia. The best-fit ellipses are calculated and the candidate grasp locations on the panel-object for the four suction cups are determined. The position control system transforms the desired grasp points from the world coordinate system to the required suction cup positions with respect to the gripper coordinate system. The suction generation system consists of a continuously operating 2.5 HP air blower. Suction is generated as a consequence of pressure differential developed within each suction unit when a panel of material is held against its surface. When the generator is operating, air flows from the atmosphere into the suction cup through perforations on its pick up surface, then through the pipes into the motor impeller casing and then out through the outlet opening of the suction generator. A 3-way diverter valve controls the activation or deactivation of suction to the RGS. By adjusting the main valves, one can regulate the amount of suction applied to the material through each of the four suction cups.

The controller testbed is shown in **Fig. 5**. The system utilizes two Compumotor AT-6400 microprocessor based 4-axes indexers that are integrated with an IBM Workstation. The position controller uses four stepper motors for positioning of the suction cups, and the suction controller uses four stepper motors to regulate suction through each of the four suction cups by controlling the corresponding regulating valves. The angular position of each motor is sensed

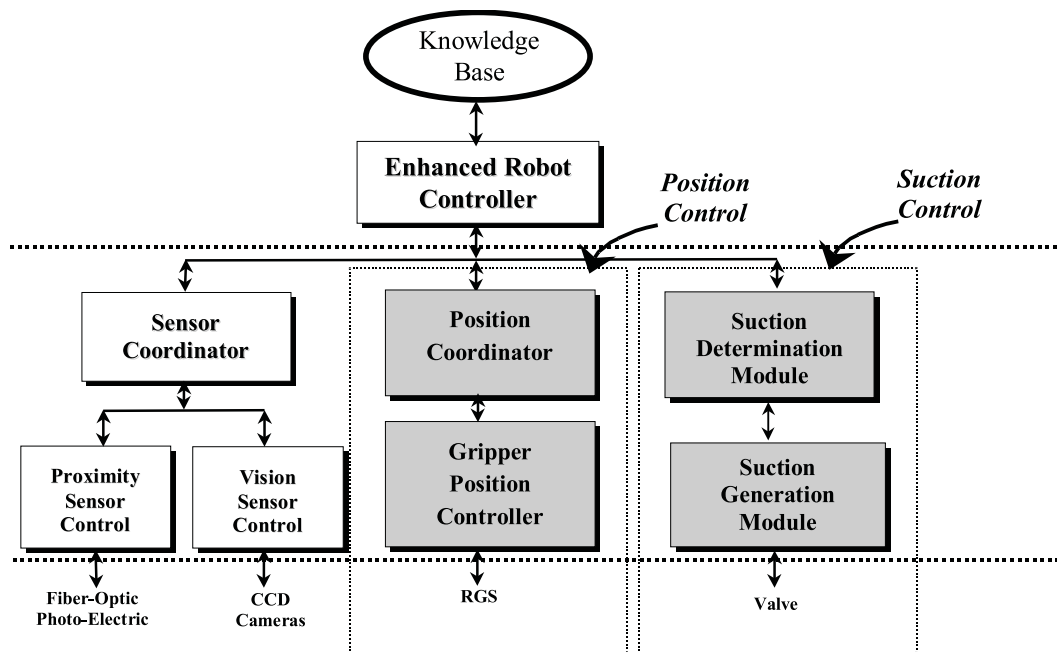


Fig. 4 The RGS hierarchical control architecture

using the shaft encoder. The indexer sends the “move” signals to the driver to control the motor motion. The indexer has a 2 millisecond update frequency and capabilities for encoder feedback and motor position capture for accurate positioning. The driver receives step input signals from the indexer and converts them to motor currents to drive the motor. The stepper motor converts the digital input signals into fixed mechanical motion increments. The encoder serves as a position verification device that feeds back the extent and the direction of motion. Matlab’s *Fuzzy Logic Toolbox* [8] running on a PC Workstation is used to generate the high level instructions to control the motor movements.

It has been experimentally found that the suction required for material manipulation depends on *Porosity* (Π) and *Weight* (W) of the material, *Robot Speed* (U), and *Distance of Travel* (D). The robot’s speed is an important factor for the determination of the ideal holding force that is achieved by regulating the airflow through the four valves of the RGS. A fuzzy logic based controller has been implemented to regulate, coordinate and maintain the amount of suction generated through each of the suction units, and the positioning of the suction cups along the length of each of the axes of the reconfigurable gripper.

3. Position Control

The suction cup is translated along the arm under the control of an actuating mechanism. The linear actuator drive mechanism consists of a lead screw, an aluminum carriage and polyacetal nut, and a ball rail and end plates. The lead screw drives the carriage and the polyacetal nut on which the suction cup is mounted. The length of the lead screw is 12 inches and it has a diameter of 0.5 inch. The positioning accuracy of the lead screw is achieved by using acme threads. Acme threads have a very low lead angle, minimizing backlash.

The stepper motor, mounted underneath the tool flange

of the robot, generates the torque required to move the linear actuator. The selection of the actuating mechanism is based on the amount of torque needed to move the suction cup along the length of the arm. The torque required to move the load, T_{sys} , is given by:

$$T_{sys} = [T_{acc} + T_{friction}] FS \quad (1)$$

where T_{acc} is the torque to accelerate the load, $T_{friction}$ is the torque required to overcome the effect of friction, and FS is the factor of safety. It has been found that in order to actuate the suction cup, a motor that generates a torque of 22.90 oz-in or higher is needed.

The stepper motor controller determines the magnitude and direction of the required displacement of the suction cups on each of the four axes. The movement of each suction cup may be controlled either independently or in a coordinated manner, to perform effective material manipulation of various shapes.

Let y_d be the desired position of each suction cup, and y_c the actual position of the cup. Then the position control formulation for each of the four cups is described by the following equations:

$$e(k) = y_d(k) - y_c(k) \quad (2)$$

$$\Delta e(k) = e(k) - e(k-1) \quad (3)$$

$$g(k) = G[e(k), \Delta e(k)] \quad (4)$$

$$u(k) = u(k-1) + g'(k) \quad (5)$$

$e(k)$ is the tracking error at time k , $\Delta e(k)$ is the change of error, and $u(k)$ is the control action. The term $G[e(k), \Delta e(k)]$ represents a nonlinear mapping as described by the fuzzy If-Then rule-base, and $g'(k)$ is the position correction given by the fuzzy inference. The derivation of $g'(k)$ is described in what follows in term of the standard terminology of fuzzy logic systems ([7],[10]). The mapping G is formally represented by rules of the

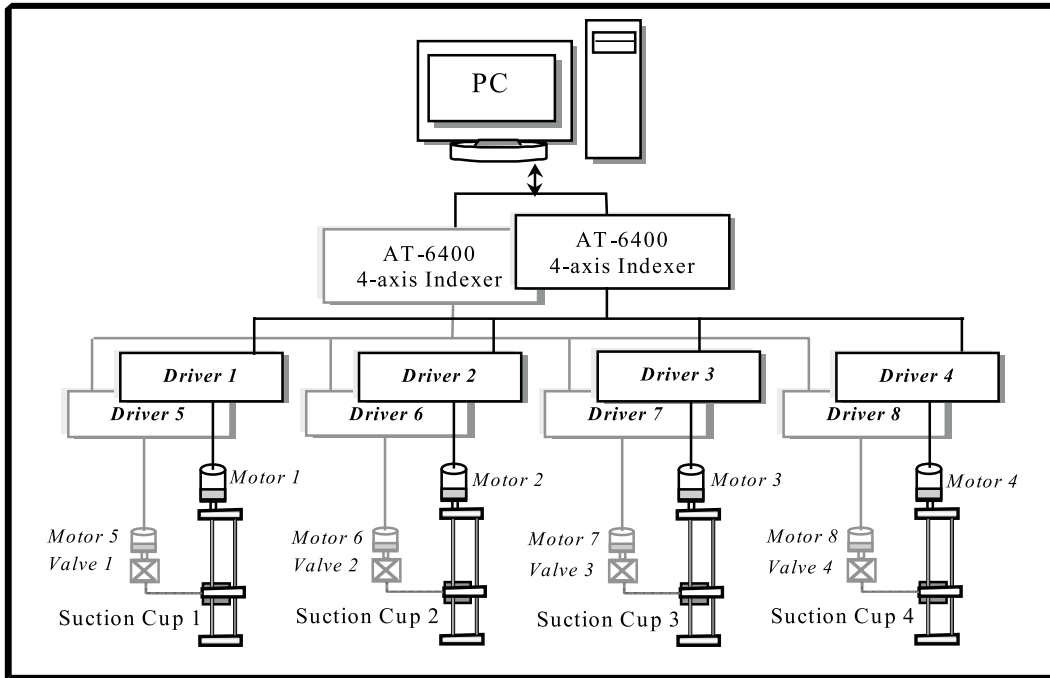


Fig. 5 Testbed for the overall position and suction control system

form:

$$\text{IF } e(k) \text{ is } T_e \text{ AND } \Delta e(k) \text{ is } T_{\rho e} \text{ THEN } g(k) \text{ is } T_g \quad (6)$$

where T_e , $T_{\rho e}$ and T_g are the linguistic term sets of $e(k)$, $\Delta e(k)$, and $g(k)$, respectively. Since the inputs of Eq. (6) are crisp measurements, a *fuzzification* process is needed, i.e., transformation of input readings into fuzzy sets. By assuming that ce and $c\Delta e$ are the fuzzified input readings, the correction g' is determined by:

$$g' = F_{\rightarrow}[(ce, c\Delta e), (e, \Delta e, g)] \quad (7)$$

where F_{\rightarrow} represents a fuzzy inference method. Equation (7) combines the actual values of error and change of error with the heuristic knowledge included in (6). Applying the *max-min compositional inference* [7] on the membership functions domain of Eq. (7), we have:

$$\mu_{g'}(y) = \max_x \min[\mu_{ce, c\Delta e}(x), \mu_{e, \Delta e, g}(x, y)] \quad (8)$$

where $\mu_{g'}(y)$ is the membership grade of the position correction, $\mu_{ce, c\Delta e}(x)$ is the membership grade of the fuzzified observation, and $\mu_{e, \Delta e, g}(x, y)$ is the membership grade of the fuzzy implication. It is necessary to compute the value of $g'(k)$ of Eq. (5). Since $g'(k)$ is a real number, $\mu_{g'}(y)$ should be *defuzzified*, as follows:

$$g'(k) = \frac{\sum y \mu_{g'}(y)}{\sum \mu_{g'}(y)} \quad (9)$$

Equation (9) determines $g'(k)$ as the center of the area within the combined membership function $\mu_{g'}(y)$. Based on this formulation, it is possible to simultaneously and independently control the individual positions of each of the four suction units. It should be noted that the actual position accuracy is based on the number of threads of the lead screw and the resolution of the driver.

4. Suction Control

The valve controller is schematically presented in **Fig. 6**. The suction generator is connected to the RGS, via a series of pipes terminating in a hub, mounted on the outer joint of the robot (as shown earlier in Fig. 3). From this central hub, flexible hoses are used to attach to the four suction cups. A valve integrated with each of the four hoses may be used to independently regulate suction to each of the four units. The valves are integrated with the enhanced robot controller which determines the amount of suction and activation or deactivation of suction through each of the suction cups. In order for the system to perform reliably, the grasp needs to be stable. It is necessary that the suction generated be greater than the weight of the material and overcome the shear forces due to robot accelerations to guarantee grasp stability.

The airflow (and consequently the suction force) is adjusted through the main valves. In the fluid mechanic analysis presented in the sequel, one can see that the simultaneous control of the four valves is nonlinear with coupled parameters involved. Further, some of the parameters cannot be accurately modeled. Thus, control methodologies that require accurate mathematical modeling of the suction system are not appropriate. On the other hand, knowledge-based formulation has been proven to work effectively in real-world systems, and it is recommended [7], [10]. Before discussing these issues, we briefly present the forces acting on each of the cups and the material.

Consider that the robot arm accelerates at a rate of a_x and a_y in the horizontal and the vertical directions, respectively. The equilibrium of forces in the horizontal and vertical directions, as shown in **Fig. 7**, may be resolved as follows:

$$\sum F_x = -F_f = ma_x \quad (10)$$

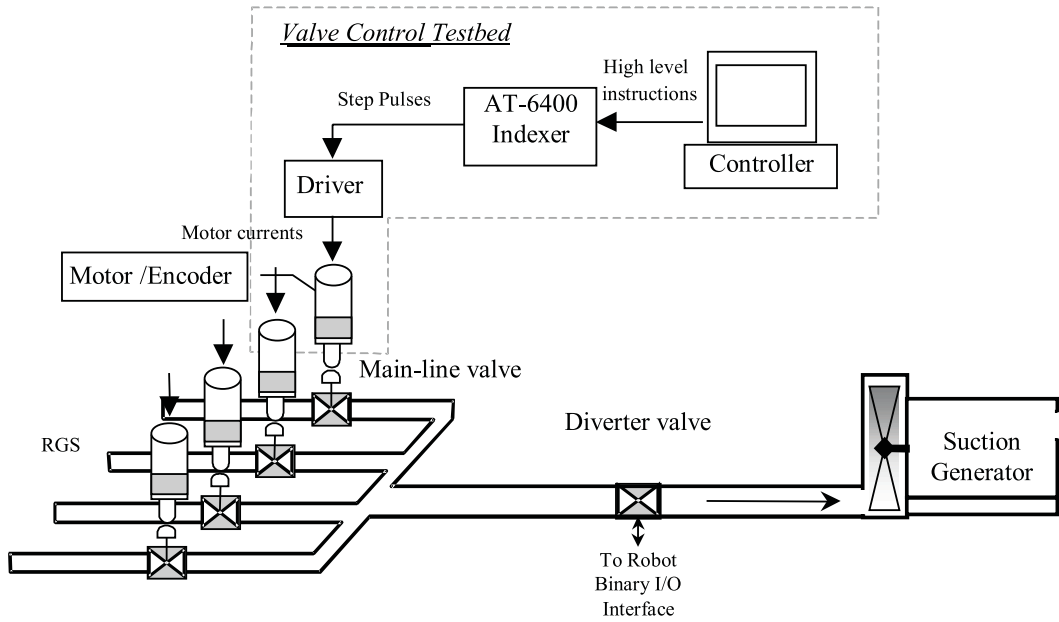


Fig. 6 Schematic of the suction control system

$$\sum F_y = P_g - W - N = ma_y \quad (11) \quad \text{equation:}$$

$$P_1 + \frac{1}{2}\rho c_1^2 + \Delta P_{imp} = P_2 + \frac{1}{2}\rho c_2^2 + \Delta P_{loss} \quad (12)$$

where, m is the mass and W is the weight of the material. The frictional force F_f holds the material on the suction unit during the translation in the horizontal plane. The value of the normal force N is determined by the equilibrium of forces in the vertical plane. Consequently, the magnitude of F_f , is determined by the equation, $F_f = \mu N$, where μ is the coefficient of friction.

For grasp stability, it is necessary that $F_x \leq \mu N$. The suction force, P_g generated at the suction unit must be sufficient to overcome the slippage effect due to the acceleration of the robot arm, and also the weight and slippage of the material, as computed using Eqs. (10) and (11). Further, these equations may be used to determine the minimum effective area of the suction unit, based on the known suction generation capabilities of the generator. As mentioned, a 2.5 HP blower, capable of generating 6.0 inches of Hg of suction has been selected. Assuming no losses, it is found that in order to handle the desired payload, the minimum effective area of suction is 5.3 [in²].

The above formulation assumes no suction losses due to air leaks, material porosity, etc., making the physical model of the system overly simplistic and unrealistic. These parameters, though experimentally measurable, are difficult to be incorporated into the mathematical model of the system. This is shown next, where an analytic modeling of the air flow through the pipe lines of the RGS, has been presented.

The generalized Bernoulli equation (Energy equation) is used for the calculation of the fluid flow through pipes, along a streamline, for steady state conditions and incompressible flows. Assuming a streamline, starting from a distance of the suction entrance (Fig. 8), at a point where air is at rest, going through the pipe line and ending at the impeller's outlet, we have from the generalized Bernoulli's

where ρ is air density, c is the mean flow velocity, ΔP_{imp} is the total pressure rise inside the impeller, ΔP_{loss} is the total pressure loss along the pipe, with point (1) corresponding to the starting point of the streamline and point (2) to the impeller's outlet (Fig. 8). In Eq. (12) the gravitational terms have been neglected, due to the small elevation and the low density of air.

The static pressure at points (1), (2) is the atmospheric pressure P_{at} , while velocity c_1 is equal to zero, as the air is at rest at the corresponding position. Consequently, Eq. (12) becomes (for each branch i):

$$\Delta P_{imp} = \frac{1}{2}\rho c_2^2 + \Delta P_{loss} = \frac{1}{2}\rho c_2^2 + \Delta P_0 + \Delta P_i \quad (13)$$

where the total pressure loss inside the pipe is analyzed in two parts. The first corresponds to the main pipe (ΔP_0) and the second to the branch (i) of the suction device (ΔP_i) (i takes values from 1 to 4). The pressure losses inside a pipe can be *linear* (or *major*) losses, due to the friction with the pipe's internal surface, and *local* (or *minor*) losses, which are associated to the irregularities of the flow in the various special parts of the pipe (bends, valves, porous media, angles, joints, etc.). All losses are functions of the square of the mean velocity (or volume flow rate). Assuming constant pipe diameter in each part (main pipe and branch i) and introducing the analytical expressions for the two kinds of losses, Eq. (13) becomes:

$$\Delta P_{imp} = \frac{1}{2}\rho c_2^2 + \left(f_0 \frac{L_0}{D_0} + k_0 \right) \frac{1}{2}\rho c_0^2 + \left(f_i \frac{L_i}{D_i} + k_i \right) \frac{1}{2}\rho c_i^2 + \Delta P_{suci}. \quad (14)$$

By rewriting Eq. (14) as a function of the corresponding volume flow rates Q_0 and Q_i (with E denoting the various

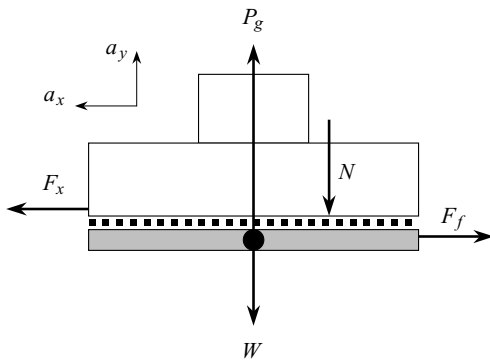


Fig. 7 Forces acting on the material during vertical and horizontal motion

pipe cross-section areas), we have

$$\Delta P_{imp} = \frac{1}{2}\rho \left(\frac{Q_0}{E_{out}} \right)^2 + \left(f_0 \frac{L_0}{D_0} + k_0 \right) \frac{1}{2}\rho \left(\frac{Q_0}{E_0} \right)^2 + \left(f_i \frac{L_i}{D_i} + k_i \right) \frac{1}{2}\rho \left(\frac{Q_i}{E_i} \right)^2 + \Delta P_{suc_i} \quad (15)$$

where $i = 1, 2, 3, 4$, f_0 and f_i are the friction factors of the main pipe and the corresponding branch (complex empirical functions of Reynolds number and the relative roughness of the internal pipe surface), L_0 and L_i are the corresponding pipe lengths, while D_0 and D_i are the corresponding pipe diameters. Minor losses are determined by k_0 and k_i , which are the sums of the local loss coefficients. These two last coefficients are complex empirical functions of the Reynolds number ($Re = cD/\nu$, c : velocity, D : diameter, ν : kinematic viscosity) and the geometry of the parts (bends, joints, etc.). The last term ΔP_{suc_i} corresponds to the pressure losses due to the porous media and the position of the control valve, and can also be modeled as:

$$\Delta P_{suc_i} = k_{suc_i} \frac{1}{2}\rho c_i^2 = k_{suc_i} \frac{1}{2}\rho \left(\frac{Q_i}{E_i} \right)^2, \quad i = 1, \dots, 4 \quad (16)$$

where k_{suc_i} is the local loss coefficient, determined by material characteristics and valve position. It should be noted that, in contrast to the other terms of the right part of Eq. (15), which can be adequately modeled (theoretically or using experimental data), ΔP_{suc_i} is highly varying and extremely difficult to be modeled with an adequate generality.

The total pressure rise inside the impeller (for a constant rotating speed) is a nonlinear function of the total volume flow rate Q_0 given by

$$\Delta P_{imp} = F(Q_0) \quad (17)$$

where F is the characteristic function of the impeller's performance and can be experimentally evaluated.

Equations (15) and (17) are coupled with the continuity equation

$$Q_0 = \sum_{i=1}^4 Q_i = Q_1 + Q_2 + Q_3 + Q_4 \quad (18)$$

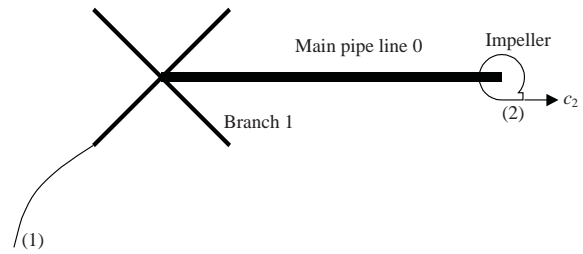


Fig. 8 Schematic representation of the pipe system

and result in a system of six nonlinear equations. By solving this system one can compute the five different flow rates and the pressure rise inside the impeller, provided that all the loss coefficients are modeled. It must be emphasized that the loss coefficients are also implicit functions of the flow rates, due to the connection of Reynolds number with the flow velocity.

Equation (18) shows that the flow rates in each branch of the pipe are coupled. Further, the pressure losses in each branch ΔP_i are also coupled, as can be seen by subtracting the four Bernoulli equations (as given in Eq. (13) or Eq. (15)):

$$\Delta P_1 = \Delta P_2 = \Delta P_3 = \Delta P_4 = \left(f_i \frac{L_i}{D_i} + k_i \right) \frac{1}{2}\rho c_i^2 + \Delta P_{suc_i}. \quad (19)$$

A change in the flow rate causes a change in the pressure losses ΔP_{suc_i} at the corresponding branch, as Eq. (16) indicates. Additionally, in order to satisfy the system of six equations, changes in the flow rates and pressure losses at the other branches are produced (including ΔP_{suc_i} , which in practice indicates how closed or opened the valve is). By closing one of the valves (in order to reduce the suction force) the suction forces in the other three branches are increased, due to the increased flow rate. This effect must be manipulated, using the corresponding actuators in order to close the three valves. Consequently, valve positions are highly and nonlinearly connected to each other and a change in the position of a valve must be followed by changes in the positions of the other three valves, provided that a desired suction level (which may be different at each branch) has to be achieved.

The control problem is to model the interactions between valves' positions and the corresponding pressure fluctuations due to the variation of valves' positions. As mentioned above, this is a nonlinear problem with coupled components for which we employ fuzzy logic modeling. The knowledge base contains some simple facts in an IF-THEN rule form. For example:

IF the pressure error is *negative big*
AND the change of the error is also *negative big*
THEN *open* the valve fast

where the expressions *negative big* and *open fast* are appropriately selected membership functions. Details on the fuzzy logic controller architecture can be found in [1], [5].

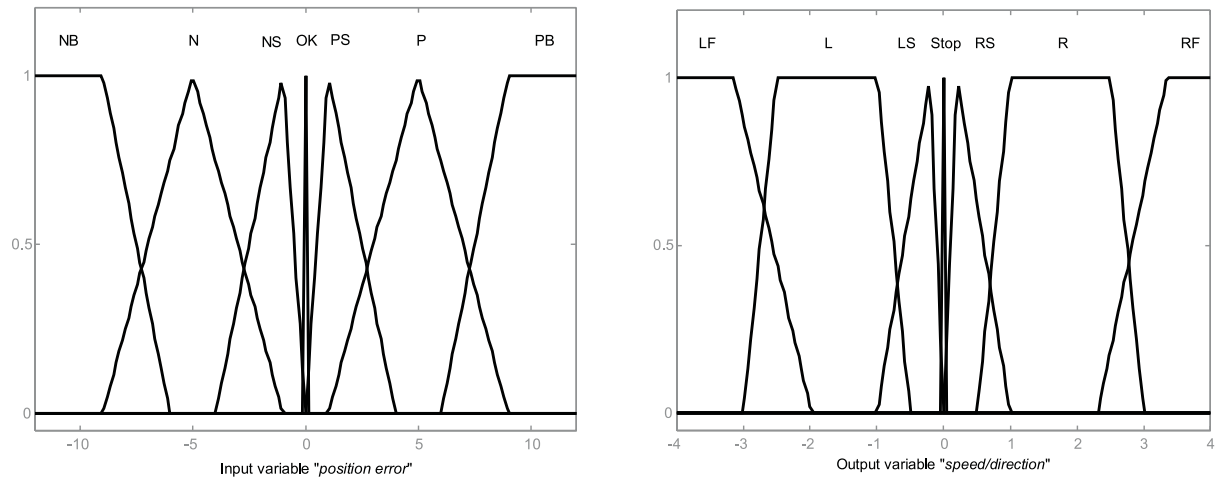


Fig. 9 Membership function plots, where for position error, NB: negative big; N: negative; NS: negative small; PS: positive small; P: positive; and PB: positive big, whereas for speed/direction, LF: left fast; L: left; LS: left slow; RS: right slow; R: right; and RF: right fast

5. Testing and Results

5.1 Position control

The suction cups are independently translated along each arm towards the goal position. The use of stepper motors with shaft encoders simplifies the implementation of the positioning control since the position error is calculated every time instant from the information given by the encoders and the proximity sensors mounted on each suction cup. Details on the sensor-based positioning algorithm for the existing gripper prototype shown in Fig. 1, can be found in [4].

Each cup's translation profile contains an acceleration period at the beginning of the motion and a deceleration one at the end. The acceleration rate depends on the position error and described by fuzzy rules, as for example:

IF the position error is *positive big*
 AND the change-of-error is *negative big*
 THEN *move right fast*.

Similarly when the "error is negative" the controller changes the direction of motion and the suction cup "moves left" towards the target point. The corresponding membership functions are shown in Fig. 9.

The position controller's rule-base is similar to the one created for the control of the main suction valve. The interested reader is referred to [1], [5].

5.2 Suction control

It has been experimentally found that the suction required for material manipulation depends on the following parameters: 1) *Porosity* (Π) and 2) *Weight* (W) of the material, 3) *Robot Speed* (U), and 4) *Distance of Travel* (D).

Once the RGS suction units are aligned with the desired grasp locations on the object, suction is activated through the suction cups, in order to enable material manipulation. This operation is governed by the overall suction control

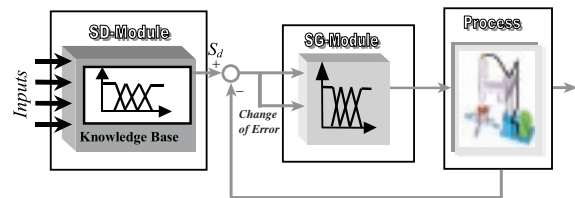


Fig. 10 Schematic of the RGS suction controller

system, which consists of two modules as shown in Fig. 10: i) The *Suction Determination* (SD) module; and ii) The *Suction Generation* (SG) module.

SD-module is an off-line process that is used to determine the amount of suction, based on the above mentioned material and plant characteristics as inputs, whereas the SG-module is an on-line component that achieves the value of the desired suction, as determined by the SD-module [5]. It is the responsibility of the SG-module to attain and maintain this value, by simultaneously adjusting the four valves.

Simulation results obtained using MATLAB'S SIMULINK simulation software find that all four suction cups reach their respective desired set points without any major overshoot or error (Fig. 11). In Fig. 11(a), all suction cups have to achieve and maintain the same amount of suction (dotted line). In practice this corresponds to a material with constant porosity and weight. Further, the distance from the center of the RGS should be the same for all suction cups. A more complicated case is shown in Fig. 11(b). Each cup has to achieve different levels of suction: 0.1, 0.3, 0.5 and 0.75 respectively. Indeed, based on object parameters (geometry, porosity, etc.), it may be possible that different values of suction are needed through the four cups. It can be seen that by opening a valve the suction force is increased at this suction cup, and the same moment is decreased at the other three cups (since the blower works at a constant rate). Because of the fact that all suction cups use suction from the same generator, the problem

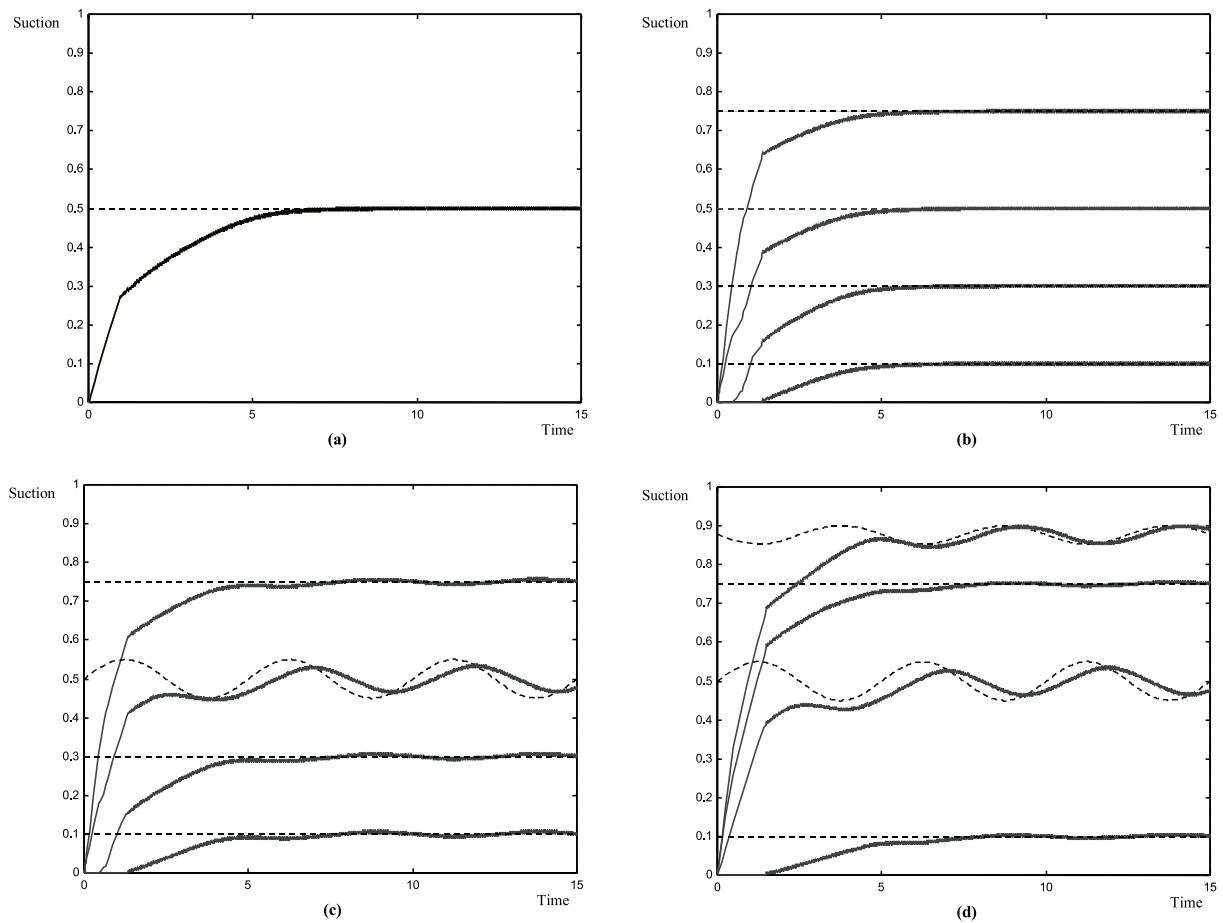


Fig. 11 Simulated performance of the 4-valve controller for various set-points

becomes highly coupled, as evident from the figures and was expected after the Bernoulli equation analysis. The interactions can be clearly seen in Fig. 11(c) and 11(d). The sinusoidal set-points in these figures may be attributed to the external disturbances due to robot's movement. The oscillations in the controller's output are due to the selected simulation accuracy and step size. However, the amount of fluctuation is very minor and considered satisfactory for the purpose of material manipulation. In all figures, suction is normalized and time is measured in seconds.

The behavior of the fuzzy controller is compared to a PID controller as shown in Fig. 12. The PID jumps faster to the set point but causes overshooting in three valves (Fig. 12(c)) while the fourth valve remains closed. This results in poor grasp stability since only three cups pick the object for almost 5 seconds. With the fuzzy controller all four cups simultaneously pick the object, as shown in Fig. 12(a). It should be noted that the PID gains were experimentally tuned by trial and error, since no analytical methods are available to determine the parameters of PID controllers. Figures 12(b) and 12(d) present the process errors for the fuzzy and PID controller respectively.

6. Conclusions

A knowledge-based control system has been designed to control the position of the four independent degrees-of-freedom of the robot gripper system (RGS), and also to control the amount of suction applied to the material

through the suction cups. The position controller uses sensory and motor feedback to accomplish positioning of the suction cups on the object at the desired grasp locations. The suction controller, first determines the amount of suction needed for material manipulation, and then, generates and maintains suction at the desired level. The performance of the control system has been simulated and validated using MATLAB software.

The overall reconfigurable gripper system has been proven to be capable of reliable and rapid manipulation of limp material without causing distortion, deformation and/or folding of the material. A major limitation of the RGS is that because of its rectangular cross-bar configuration, it can handle only a limited number of geometrical shapes and sizes of objects. Further designs will be investigated into, as necessary.

Acknowledgments

This work was partially supported by Louisiana Educational Quality Support Fund, Industrial Ties Research Subprogram grant LEQSF (1996–1999)-RD-B-14, and National Science Foundation, Design, Manufacturing and Industrial Innovation grant NSF-DMII-9701533.

References

- [1] N. Tsourveloudis, R. Kolluru, K. P. Valavanis, and D. Gracanic, "Suction control of a robotic gripper: a neuro-fuzzy approach," *Journal of Intelligent and Robotic Systems*, vol. 27, no. 3, March 2000, to be appeared.

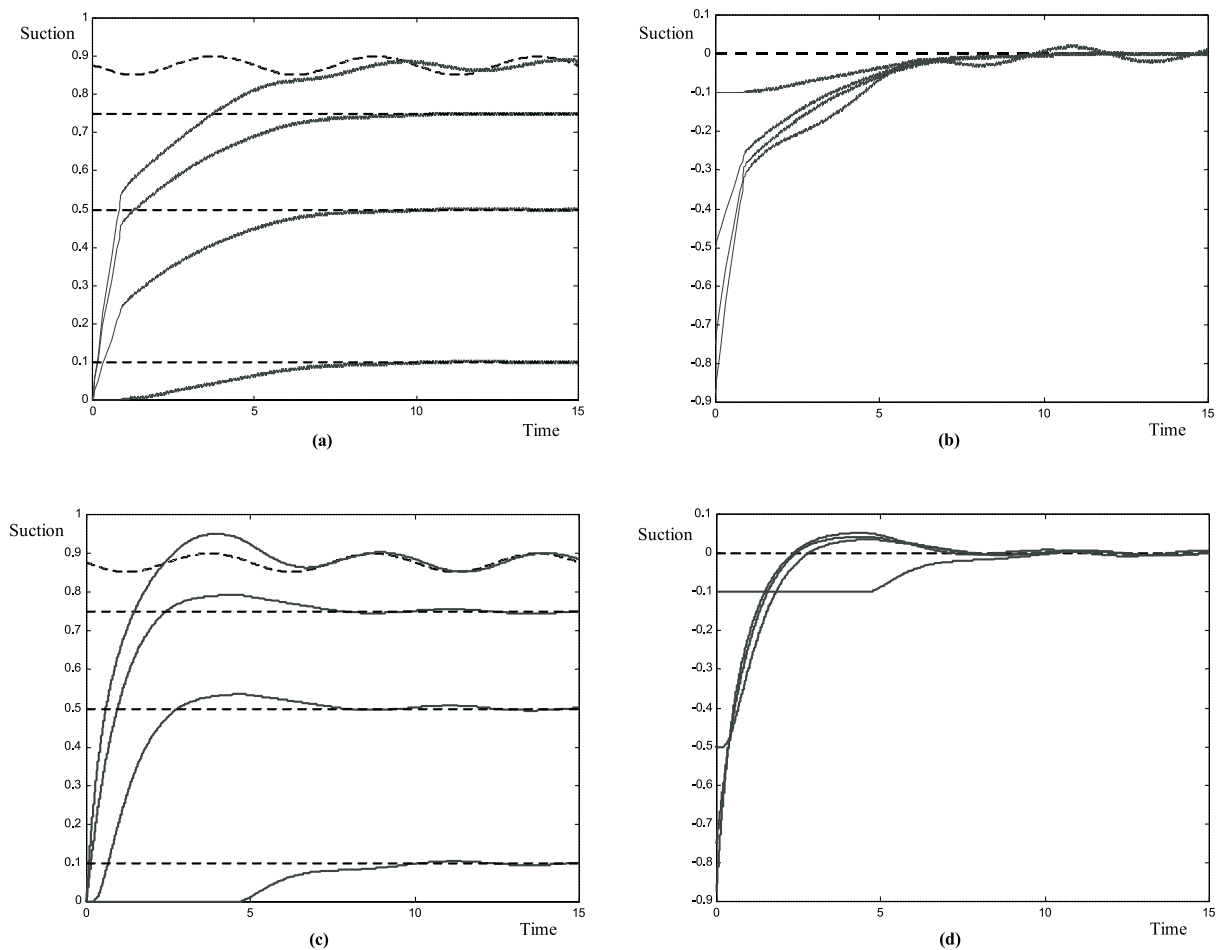


Fig. 12 Fuzzy and PID controller's performance and error comparison

- [2] R. Kolluru and K. P. Valavanis, "Modeling, analysis and performance evaluation of a robotic gripper system for limp material handling," *IEEE Trans. on Systems, Man and Cybernetics*, vol. 28B, no. 3, pp. 480–486, June 1998.
- [3] R. Kolluru, K. P. Valavanis, A. Steward, and M. J. Sonnier, "A flat surface robotic gripper for handling limp material," *IEEE Robotics and Automation Magazine*, vol. 2, no. 3, pp. 19–26, September 1995.
- [4] T. Hebert, K. P. Valavanis, and R. Kolluru, "A real-time, hierarchical sensor-based robotic system architecture," *Journal of Intelligent and Robotic Systems*, vol. 21, no. 1, pp. 1–27, January 1998.
- [5] N. C. Tsourveloudis, R. Kolluru, and K. P. Valavanis, "Fuzzy control of suction-based robotic gripper system," in *Proc. of the IEEE International Conference on Control Applications*, Trieste, Italy, 1998, pp. 653–657.
- [6] J. E. Shigley, *Mechanical Engineering Design*. New York, NY: McGraw-Hill, 3rd edition, 1997.
- [7] D. Driankov, H. Hellendoorn, and M. Reinfrank, *An Introduction to Fuzzy Control*. Berlin, Germany: Springer-Verlag, 2nd edition, 1996.
- [8] *Fuzzy Logic Toolbox User's Guide*. Natick, MA: The MathWorks, Inc., 1998.
- [9] W. T. Thomson, *Theory of Vibration with Applications*. Englewood Cliffs, NJ: Prentice-Hall, 3rd edition, 1988.
- [10] D. Dubois and H. Prade, *Fuzzy Sets and Systems: Theory and Applications*. New York, NY: Academic Press, 1980.
- [11] M. H. Lawry, *I-DEAS Master Series Mechanical CAE/CAD/CAM Software*. OH: Structural Dynamics Research Corporation (SDRC), 1993.
- [12] R. Kolluru, K. P. Valavanis, N. Tsourveloudis, and S. Smith, "Design fundamentals of a reconfigurable robotic gripper system," *IEEE Trans. on Systems, Man and Cybernetics*, vol. 30, no. 2, March 2000, to be appeared.

Biographies

Nikos Tsourveloudis received the diploma and Ph.D. degrees in production engineering and management from the Technical University of Crete, Chania, Greece, in 1990 and 1995, respectively. From 1992 to 1995, he was the president of the Hellenic Association of Industrial Engineers. From 1996 to 1998, he was a visiting research scientist at the Robotics and Automation Laboratory, A-CIM Center, University of Southwestern Louisiana, Lafayette, LA, USA. Currently he is an adjunct professor at the Department of Production Engineering and Management of the Technical University of Crete. His research interests lie in the areas of fuzzy control, modeling of flexible manufacturing systems, planning, scheduling, integration of production networks, and autonomous operation/navigation of unmanned vehicles. Dr. Tsourveloudis received the Best Student Paper Award of the manufacturing division of the 3rd World Automation Congress, held in Anchorage, Alaska, in 1998.

Kimón P. Valavanis received the Diploma in Electrical Engineering from the National Technical University of Athens, Athens, Greece, in 1981, and the M.Sc. and Ph.D. degrees in Electrical Engineering, Computer and Systems Engineering from Rensselaer Polytechnic Institute, Troy, NY, in 1984 and 1986, respectively. Since 1991 he has been with The Center for Advanced Computer Studies, University of Louisiana at Lafayette (former University of Southwestern Louisiana), where he is a professor of computer engineering and the director of the Robotics and Automation Laboratory. He is also the A-CIM/BORSF Regents Professor of Manufacturing. His research interests are in the areas of robotics, automation, and distributed intelligence systems. Currently (academic year 1999–2000) he is with the Technical University of Crete, Greece, Department of Production Engineering and Management. He has published more than 180 technical papers, book chapters, and technical reports. He has been the general chair and the program chair of IEEE conferences and symposia, and an editor of several conference proceedings. He is also an Editor-in-Chief of the IEEE Robotics and Automation Magazine. Dr. Valavanis is a Senior Member of IEEE.

Ramesh Kolluru is the Associate Director of Research for the A-CIM Center, and an adjunct Assistant Professor with the Center for Advanced Computer Studies. His research expertise spans the areas of flexible and agile manufacturing systems, intelligent machines, distributed database technologies, distributed and networked systems. He is currently involved in the development of intelligent machines for automated manufacturing. His research has resulted in design and development of robotic systems to automate limp material handling. Dr. Kolluru's research has been funded by federal and state agencies and the private sector. He has published extensively in such journals as the IEEE Journal of Intelligent and Robotic Systems, IEEE Transactions on Systems, Man and Cybernetics, IEEE Conference on Robotics and Automation, etc. He is the Associate Editor of the International Journal of Agile Manufacturing, and serves on the Advisory Committee of the International Journal of Advanced Manufacturing Systems.

Ioannis K. Nikolos received the diploma degree in Mechanical Engineering from the National Technical University of Athens (N.T.U.A.) in 1990, and the Ph.D. degree in Fluid Mechanics (Lab. of Thermal Turbomachines) from the Mech. Eng. Dept. of N.T.U.A in 1996.

From October 1998 he is an adjunct Lecturer with the Department of General Studies and the Department of Production Engineering and Management of the Technical University of Crete, Chania, Greece. His research interests are in Fluid Mechanics, axial and radial compressors and turbines, pump flows and Computational Fluid Dynamics. Dr. Nikolos is a member of the Technical Chamber of Greece and the Greek Society of Mechanical Engineers.